ELSEVIER

Thermochimica Acta 342 (1999) 31–39

thermochimica acta

www.elsevier.com/locate/tca

# Determination of phase stability in a bulk amorphous alloy by differential scanning calorimetry

George W. Smith, Frederick E. Pinkerton*, Jerome J. Moleski

*General Motors Research and Development Center, Warren, MI 48090 9055, USA*

Received 19 April 1999; received in revised form 6 August 1999; accepted 17 August 1999

**Abstract**

Phase transformations in a bulk amorphous alloy have been studied by differential scanning calorimetry (DSC). DSC scans exhibited increasingly complex structure as the temperature scan rate was reduced. A Kissinger analysis yielded transformation time constants and activation energies for several peaks and also for the glass transition. The fact that the Kissinger method fits the glass transition data was surprising but justifiable. Several higher temperature peaks departed from Kissinger behavior, particularly for very low scan rates. The DSC results indicate that the amorphous phase should be stable at temperatures near and above 200°C. © 1999 Elsevier Science B.V. All rights reserved.

*Keywords:* Bulk amorphous alloy; Phase transformation kinetics; Differential scanning calorimetry; Kissinger analysis; Amorphous phase stability

## 1. Introduction

Amorphous metal alloys (metallic glasses) are formed when certain alloys are quenched sufficiently rapidly that the atoms freeze into a non-crystalline arrangement. Overcoming the tendency of conventional alloys to crystallize usually requires the extremely high cooling rates attainable only by rapid quenching such as melt-spinning. The cooling rates in this method restrict the product sample to geometries which are small in a least one dimension (e.g., ribbons ca. 30 μm thick).

Recently, a new class of glass forming alloys has emerged which can be made amorphous at much lower cooling rates with dimensions approaching or reaching several mm [1–6]. The attraction of these materials lies in the unique properties which can arise in the absence of crystalline structure: high tensile strength, high corrosion resistance, and good wear resistance are examples of possible benefits offered by some amorphous materials. Some of these materials have glass transition temperatures $T_g$ as much as 100°C lower than their crystallization temperature $T_x$. When such a material is heated to $T_g$, it changes from a glass to a supercooled liquid, its behavior is quite similar to that observed for a variety of polymers. Further heating to $T_x$ results in a transformation to the crystalline phase, a process which is accompanied by considerable heat release (i.e., an exotherm).

An aspect of considerable importance to phase stability and processing parameters regarding these materials is the question of the kinetics of the various transformations they can undergo. In the present paper we apply differential scanning calorimetry (DSC) to determine kinetic parameters (time constants, $\tau$, and

*Corresponding author. Tel.: +1-810-986-0661; fax: +1-810-986-3091.


PII: S0040-6031(99)00306-8

activation energies, $E_{act}$) for certain phase transformations. Our technique is to record DSC thermal spectra at various temperature scan rates and apply the analytic method of Kissinger [7,8] to determine $\tau$ and $E_{act}$, a procedure which Smith [9–12] has used successfully to study precipitation in aluminum alloys. In the present case some peaks departed from Kissinger behavior at low scan rates.

Several previous authors [13–17] have used scanning calorimetry to study phase transformation in amorphous or metallic glasses. Yannacopoulos and Kasap [13] determined the glass transition temperature, $T_g$, in amorphous thin film selenium at various temperature scan rates. They found non-Arrhenius behavior in their Kissinger analyses of $T_g$. Kwong et al. [14] studied crystallization in amorphous thin film $Al_{85}Y_{10}Ni_5$, noting that higher scan rates increased the number of steps involved in the crystallization process. They applied both Kissinger [7] and Ozawa [18] analyses to the crystallization process, obtaining reasonable agreement from the two theories. However, they observed departures from good fits at the higher scan rates. Busch et al. [15,16] studied $Zr_{41.2}Ti_{13.8}Cu_{12.5}Ni_{10.0}Be_{22.5}$ — a metallic glass very similar to our own material. They determined the effect of scan rate on the specific heat change at $T_g$, and on crystallization behavior. They did not apply either the Kissinger or Ozawa analysis to the scan rate dependence of the transitions, although they did fit an Arrhenius equation to the crystallization temperature. They determined the heat of crystallization to be 5.5 kJ/g-atom (92 J/g) at a heating rate of 10°C/min and found that the lower bound (Kauzmann temperature) for the kinetically observed glass transition was 560 K (287°C). They also reported that above $T_g$ and prior to crystallization, the metallic glass phase separates into two compositionally distinct amorphous regions, one Zr-rich and the other Be-rich. Crystallization proceeds first in the less thermodynamically stable Zr-rich region. Finally, Spriano et al. [17] have studied the products of crystallization in a bulk amorphous specimen similar to our own. They identified four DSC signatures which they ascribed to amorphous phase separation, crystallization (in two steps) into a phase having the hexagonal $MgZn_2$ structure type, followed at higher temperature by the appearance of a tetragonal $Ti_2Zn$-type structure. They did not apply a Kissinger-type analysis to their data.

## 2. Experimental

### 2.1. Samples

Specimens cut from rods of bulk amorphous ZrTiCuNiBe alloy were studied. X-ray diffraction, optical microscopy, and electron microprobe analysis of samples cut from the rods have confirmed their amorphous character. Their chemical composition is $Zr_{40}Ti_{13}Cu_{11}Ni_{10}Be_{26}$ as determined by inductively coupled plasma atomic emission spectroscopy (ICP/AES). The cylindrical center section of each rod was sliced using a diamond saw into samples 5.35 mm in diameter and approximately 1 mm thick, having masses, $m$, within the range 110–120 mg.

### 2.2. Differential scanning calorimetry

The phase transformation behavior in the bulk amorphous alloy was studied using a Perkin-Elmer DSC7 differential scanning calorimeter. The DSC instrument measures $dQ/dt$, the rate of heat absorption or emission by the sample, as a function of temperature, $T$ [9–12]. In the absence of thermal events, the position of the baseline in such a plot is proportional to the specific heat of the sample. The presence of an endothermic peak, superimposed on the baseline, indicates the occurrence of a heat-absorbing event such as melting. On the other hand, an exothermic peak occurs as a result of some sort of heat-releasing event such as crystallization. The area under a peak is proportional to $\Delta Q$, the heat absorbed or released by the sample over the temperature range of the peak. The calorimeter can also detect glass transitions which are characterized by a smooth step-wise increase in DSC signal.

In Fig. 1 are plotted curves of $dQ/dt$ versus $T$ for the bulk amorphous alloy for scan rates, $S$, ranging from 0.6 to 10°C/min. For clarity the DSC thermal scans are offset from one another and are normalized to $S = 1$°C/min and $m = 100$ mg. Transitions are labeled for $S = 10$°C/min, 2.5°C/min, and 1.2°C/min. In one or two cases more than one measurement at a given scan rate was carried out to check consistency of DSC results. At the highest scan rate a glass transition at $T_g$ and four exothermic peaks are visible. The total heat associated with the two major exotherms (at $S = 10$°C/min) is $\Delta Q = -79.5$ J/g, somewhat lower

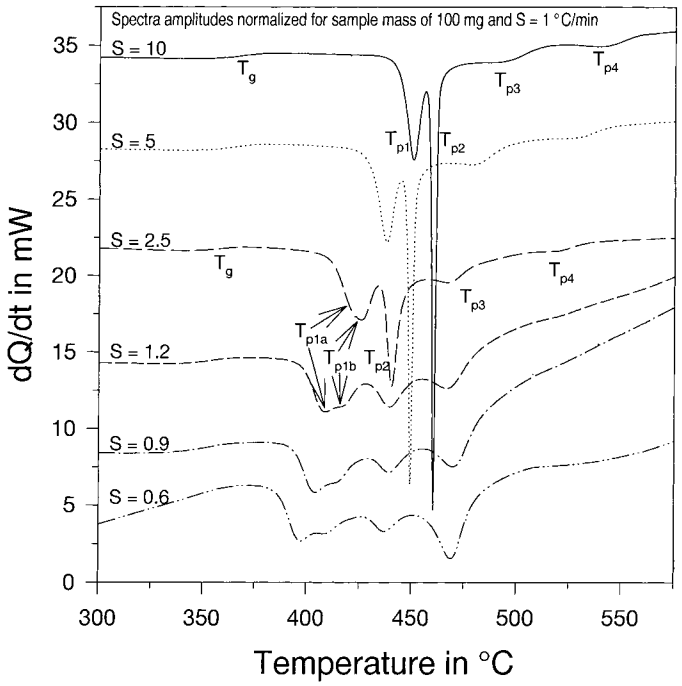


Fig. 1. Plots of d$Q$/d$t$ versus temperature for the bulk amorphous alloy. The spectra have been shifted for clarity. The glass transition and several exothermic peaks are clearly visible.

than the value for the similar alloy of Busch et al. [15]. For low scan rates the peak at lowest temperature is resolved into two components.

We refer to the DSC studies of Spriano et al. [17] on a similar $Zr_{40}Ti_{14}Cu_{10}Ni_{11}Be_{26}$ alloy to guide identification of the transformations associated with the various peaks in Fig. 1. This is made somewhat ambiguous by the observation that their DSC signatures are considerably broader and less well resolved than those we have obtained. Nevertheless, following their assignments for the DSC peaks, we can ascribe the first exothermic peak, $T_{p1}$, to the initial phase separation of the amorphous phase into two compositionally distinct Zr-rich and Be-rich amorphous phases, followed by primary crystallization into the hexagonal $MgZn_2$-type phase at $T_{p2}$. The highest temperature peak at $T_{p4}$ corresponds to the appearance of the tetragonal $Ti_2Zn$-type structure. The intermediate peak at $T_{p3}$ corresponds most closely with that described by Spriano et al. as a secondary crystallization of the hexagonal $MgZn_2$-type structure in regions not crystallized at $T_{p2}$ (perhaps the more stable Be-rich amorphous regions). This identification is subject to question, however, since Spriano et al. showed that their secondary crystallization peak merges with the primary one at scan rates of 10°C/min and above. Spriano et al. did not use scan rates below 2°C/min and therefore did not observe the splitting of the $T_{p1}$ peak evident in our results.

## 3. Kissinger analysis

Although the Kissinger analysis to derive activation energies from DSC temperature scans has been discussed previously [9–12], it is appropriate to review its salient features. The method is based on the fact that the observed temperature of a peak depends on the scan rate, $S = dT/dt$, of the experiment. Peaks for slow scan rates generally occur at lower temperatures than those for fast scan rates. Such shifts of peak temperature, $T_p$, with a change in scan rate can be seen for several exotherms in Fig. 1. Scan rates slow compared to the calorimeter response time are used in order to

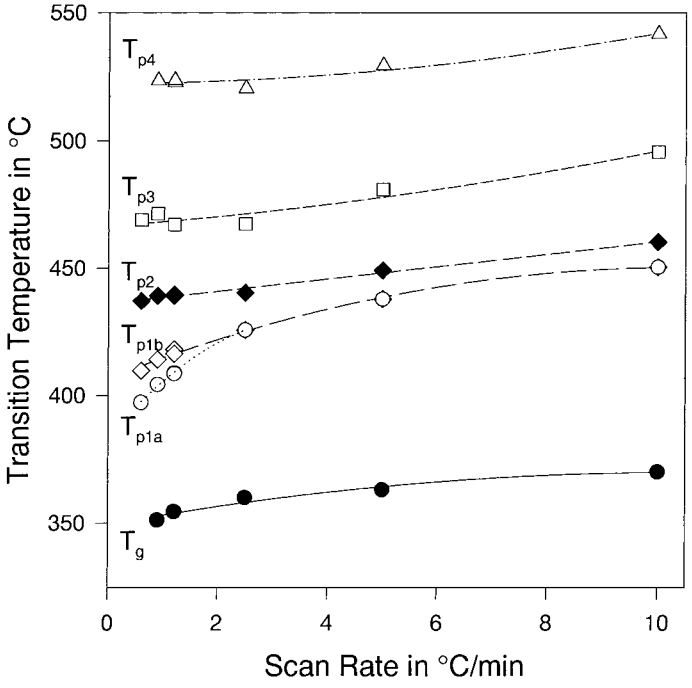


Fig. 2. Dependence of transition temperatures for the bulk amorphous alloy on temperature scan rate for the DSC experiment.

avoid time lags which shift peak temperatures to high values [9–12]. The temperatures for the transitions of Fig. 1 are plotted as a function of scan rate in Fig. 2.

The Kissinger expression, as modified by Mittemeijer et al. [8], relates $T_p$ to $S$:

$$\ln(T_p^2/S) = E_{act}/(RT_p) + \ln(E_{act}/Rk_0). \quad (1)$$

Here $E_{act}$ is the effective activation energy for the process associated with the peak, $R$ the gas constant, and $k_0$ is the pre-exponential factor in the Arrhenius equation for the rate constant $k$:

$$k = k_0 \exp(-E_{act}/RT) \quad [\text{or } \tau \equiv 1/\mathrm{k} = \tau_0 \exp(E_{act}/RT)]. \quad (2)$$

It is easy to show that substitution of Eq. (2) into Eq. (1) yields a simple expression for $k_p$, the value of $k$ at temperature $T_p$:

$$k_p = (E_{act}/R) \times (S/T_p^2) \quad [\text{or } \tau = (R/E_{act}) \times (T_p^2/S)]. \quad (3)$$

Thus the time constant from the Kissinger analysis is proportional to the exponential of Eq. (1), with a proportionality constant of $R/E_{act}$. In Eqs. (1) and (3) the units of $T_p$ are K and of $S$ are °C/s (or K/s) so that $k$ is given in $s^{-1}$.

A fundamental assumption in deriving the Kissinger equation is that the fraction, $X_p$, of species transformed at the peak temperature is independent of scan rate [19]. Although the method was originally derived to analyze peak temperatures, we shall see that it also applies to the glass transition temperature, $T_g$. This is perhaps not surprising since the glass transition temperature determined using a Perkin-Elmer [20] DSC instrument is defined to be that temperature at which the change in specific heat reaches half its maximum value (i.e., the transformation from the glassy to the supercooled liquid state is 50% complete). Thus, by definition, the fundamental assumption of the Kissinger derivation is satisfied. For peaks which strongly overlap, the applicability of the Kissinger analysis becomes more questionable. Thus, as we see in Fig. 1, the peak complexity for low scan rates ($S < 2.5$°C/min) may introduce uncertainty into the results.

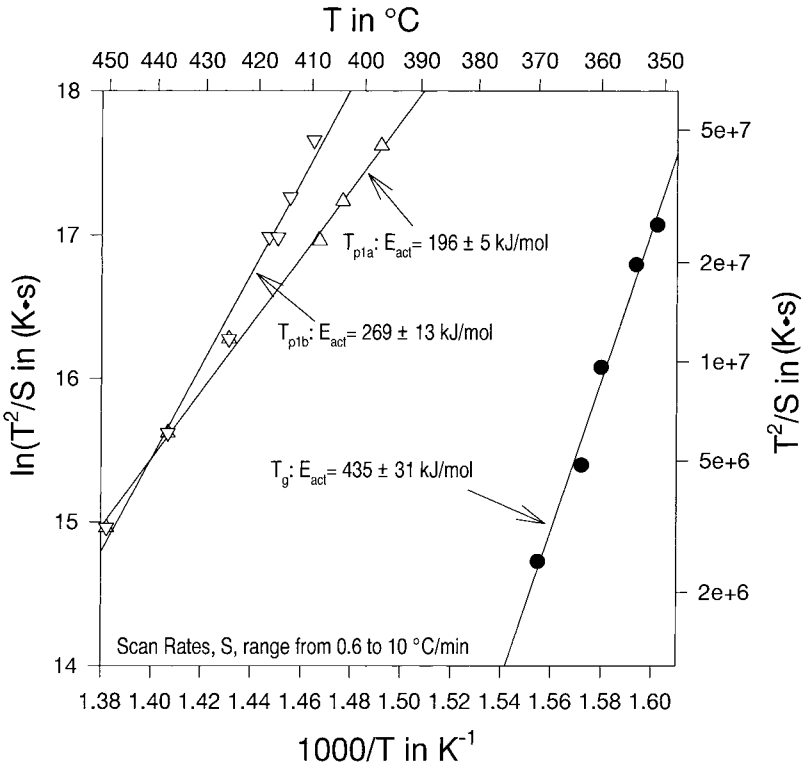


Fig. 3. Kissinger plots for the glass transition and the two components of the lowest temperature exotherm in the bulk amorphous alloy. The regressions are best fits of Eq. (1) to the data.

## 4. Analysis results

### *4.1. Glass transition (at $T_g$)*

The applicability of the Kissinger analysis to the glass transition is demonstrated in Fig. 3 where we plot a linear regression fit of Eq. (1), using values of $T_g$ derived from the DSC curves of Fig. 1. The fit is good although the activation energy (435 kJ/mol) seems high. For $S = 0.6$°C/min no data point is shown since at that low scan rate the glass transition was not readily discernible.

### *4.2. First exotherm (at $T_{p1a}$ and $T_{p1b}$)*

It is understood that the first two prominent peaks in Fig. 1 are due to crystallization of the amorphous alloy. Careful scrutiny of Fig. 1 shows that the peak labeled $T_{p1}$ for $S = 10$°C/min is resolved into two sub-peaks ($T_{p1a}$ and $T_{p1b}$) for scan rates less than 2.5°C/min. Kissinger plots for these sub-peaks are also given in Fig. 3, where it is clear that both obey Eq. (1). The activation energy for $T_{p1a}$ (196 kJ/mol) is appreciably smaller than that for $T_{p1b}$ (269 kJ/mol). These activation energies, while comparable to the value (190 kJ/mol) obtained by Kwong et al. [14] for the first of the three crystallization processes in their thin film ternary, are much smaller than the values (550 and 950 kJ/mol) for their second and third processes.

### *4.3. Second exotherm (at $T_{p2}$)*

At fast scan rates the peak labeled $T_{p2}$ (presumably also due to crystallization) is extremely sharp, but like the first peak it shifts to lower temperature as scan rate decreases, becoming broader and nearly as weak as the first peak (Fig. 1). At the very lowest scan rates ($S < 2.5$°C/min) the peak shift rate is also very small, as seen in the Kissinger plot for $T_{p2}$ (Fig. 4). Two quite different activation energies, 1596 and 289 kJ/mol, are obtained for scan rates below and above $S = 2.5$°C/min.

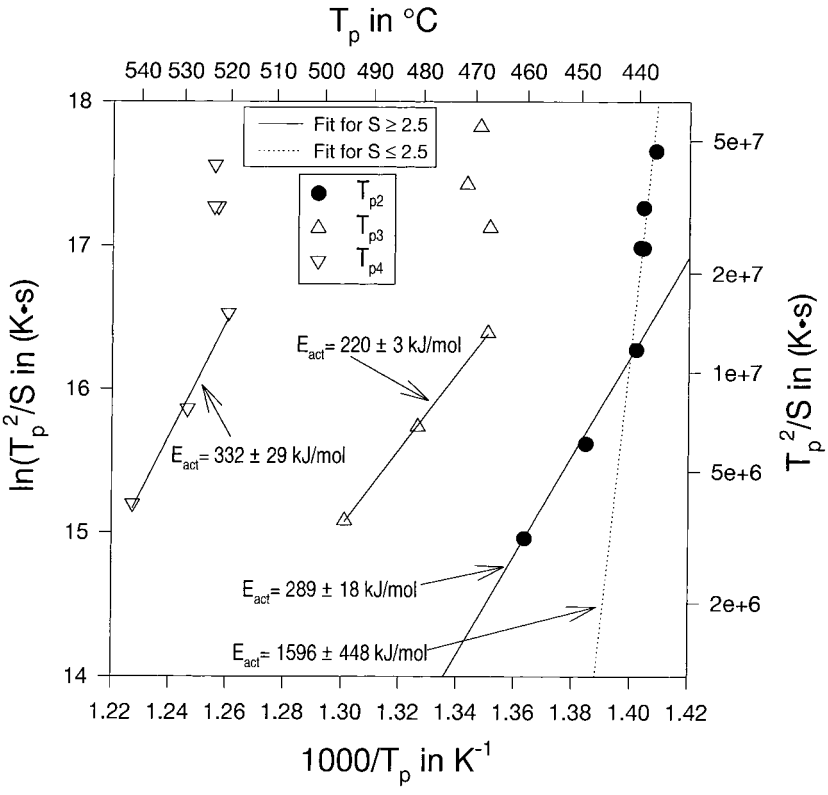


Fig. 4. Kissinger plots for the three highest temperature exotherms in the bulk amorphous alloy. It is clear that different mechanisms are responsible for the behavior of $T_{p2}$ above and below 2.5°C/min. For $T_{p3}$ and $T_{p4}$ the Kissinger relation completely breaks down at scan rates above 1.2°C/min.

### *4.4. Third and fourth exotherms (at $T_{p3}$ and $T_{p4}$)*

The third and fourth exotherms are both low and broad for $S = 10$°C/min. The mechanisms for the associated transitions are not known. The Kissinger plots for $T_{p3}$ and $T_{p4}$ in Fig. 4 are similar to that for $T_{p2}$, although at low scan rates the peak temperatures remain essentially constant. The activation energies for faster scans are 220 kJ/mol ($T_{p3}$) and 332 kJ/mol ($T_{p4}$).

## 5. Time constants from Kissinger analyses

### *5.1. Glass transition (at $T_g$)*

As seen in Fig. 5, the glass transition temperature shifts from ca. 370°C to ca. 350°C when the scan rate is reduced from 10°C/min to 0.9°C/min. The data exhibits very good Arrhenius behavior. At the lowest scan rate the glass temperature is near 350°C, and the time constant (from Eq. (3)) for the transformation from the glassy to the supercooled liquid phase is about 500 s (ca. 8 min). As scan rate decreases $\tau$ is even longer. Indeed, extrapolation of Eq. (3) indicates that at 250°C the transformation time should exceed $1.6\times10^6$ h (183 years). Only 50°C higher (300°C) the phase stability is appreciably reduced ($\tau \approx 260$ h).

### *5.2. First exotherm (at $T_{p1a}$ and $T_{p1b}$)*

The Kissinger time constants for the two components of the first exothermic peak (crystallization) are given in Figs. 6 and 7. Both plots show good Arrhenius behavior. At the lowest scan rate (0.6°C/min) the crystallization temperatures of both components are ca. 400°C, and the transformation times are near 2000 s. Extrapolation of Eq. (3) indicates that at

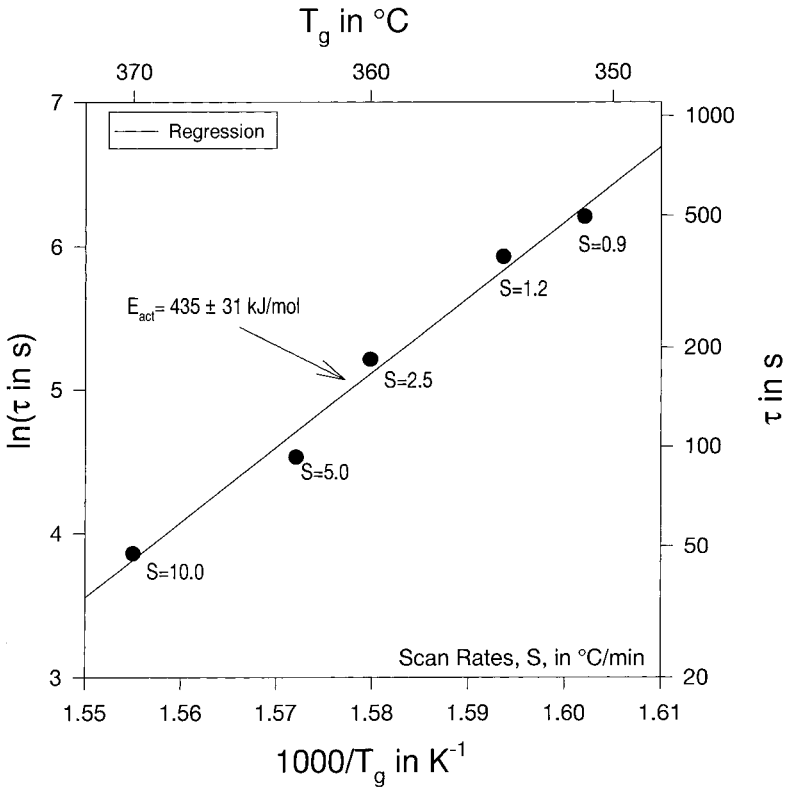


Fig. 5. Time constants for the glass transition in the bulk amorphous alloy derived from Eq. (3) under the assumption that the Kissinger analysis is valid for $T_g$.

250°C the transformation time for the peak at $T_{p1a}$ should exceed $10^4$ h (1.1 years). At 300°C, the phase stability is considerably less ($\tau \approx 200$ h). For the $T_{p1b}$ peak the transformation time extrapolated to 250°C is $\sim 7 \times 10^5$ h (80 years) which is reduced to 3000 h (0.3 years) at 300°C. Thus it appears that the lifetime of the amorphous phase can be quite long at temperatures below 250°C. However, an increase of only 50°C significantly shortens it.

### 5.3. Higher temperature exotherms (at $T_{p2}$, $T_{p3}$, and $T_{p4}$)

As already seen in Fig. 4, the Kissinger plots for these peaks exhibit abrupt changes of slope for scan rates below 2.5°C/min. The anomalous behavior of these three exotherms makes it inappropriate to apply Eq. (3) to derive $\tau$ values. It appears that different mechanisms are responsible for the fast and slow scan data. This speculation is borne out by the fact that the total heat of crystallization (of the lower temperature peaks) remains constant at ca. 80 J/g for scan rates above 5°C/min, but increases dramatically from ca. 120 to more than 170 J/g as the scan rate decreases from 2.5°C/min to 0.6°C/min.

## 6. Discussion

It is evident that the Kissinger analysis can be successfully applied only to the glass transition and the lowest temperature crystallization peak in the amorphous alloy. The time constant for the transformation from the glassy to the supercooled liquid phase is extremely large ($\geq$200 years) for temperatures below 250°C. Since crystallization must be avoided in order to preserve the desired mechanical and chemical properties of the amorphous alloy, the time

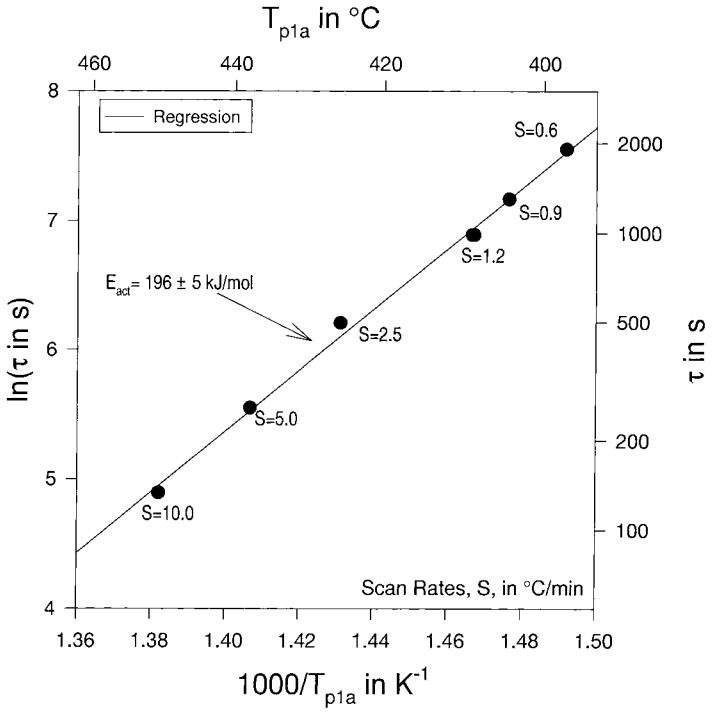


Fig. 6. Time constants (from Eq. (3)) for the first component of the lowest temperature exotherm in the bulk amorphous alloy.

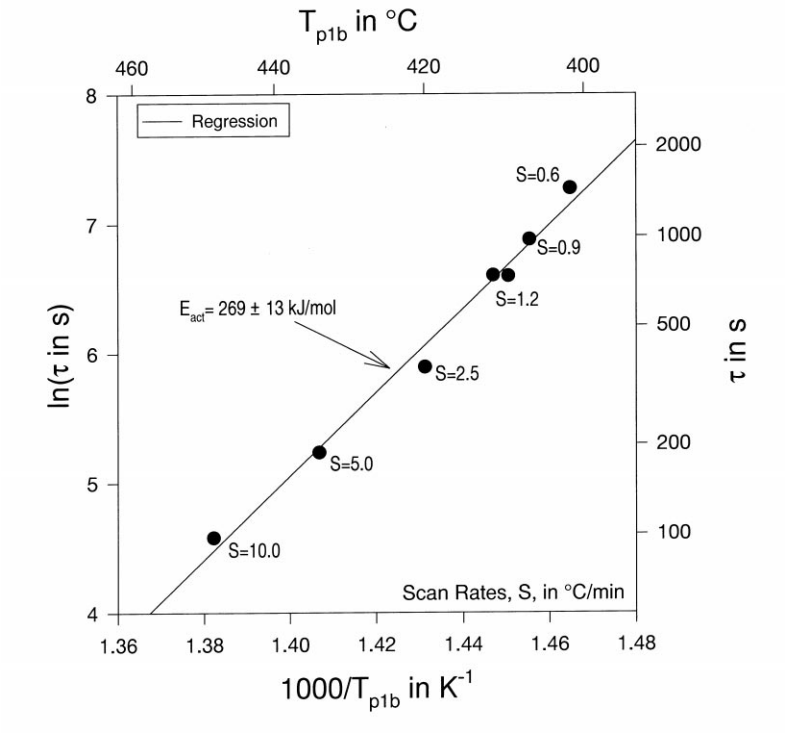


Fig. 7. Time constants (from Eq. (3)) for the second component of the lowest temperature exotherm in the bulk amorphous alloy.

constant for the first crystallization peak is of greater importance. The extrapolated lifetime of the amorphous phase at 250°C is greater than 1 year, rising rapidly with small decreases in operating temperature (to 12.6 years at 225°C and 160 years at 200°C). (These extrapolations are consistent with the Kauzmann temperature (287°C) for a similar alloy determined by Busch et al. [15].) Thus these DSC kinetic measurements indicate that the amorphous phase should be stable at temperatures up to 200°C and perhaps even higher. Finally, it should be noted that further study of the effect of scan rate on phases and grain sizes in the final crystallization products would be useful.

## Acknowledgements

The authors thank Craig Cook and George Frahm for providing the samples, Noel Potter and Deborah Esch for the ICP/AES analysis, and Jan Herbst for useful comments regarding the manuscript.

## References

[1] Y. He, G.J. Shiflet, S.J. Poon, J. Alloys Compounds 207/208 (1994) 349.
[2] A. Inoue, N. Matsumoto, T. Masumoto, Mater. Trans. JIM 31 (1990) 493.
[3] A. Peker, W.L. Johnson, Appl. Phys. Lett. 63 (1993) 2342.
[4] A. Peker, W.L. Johnson, Mater. Sci. Eng. A 179/180 (1994) 173.
[5] A. Inoue, T. Zhang, N. Nishiyama, K. Ohba, T. Masumoto, Mater. Trans. JIM 34 (1993) 1234.
[6] A. Inoue, T. Nakamura, N. Nishiyama, T. Masumoto, Mater. Trans. JIM 33 (1992) 937.
[7] H.E. Kissinger, Anal. Chem. 29 (1957) 1702.
[8] E.J. Mittemeijer, L. Cheng, P.J. van der Schaaf, C.M. Brakman, B.M. Korevaar, Metall. Trans. 19A (1988) 925.
[9] G.W. Smith, Thermochim. Acta 313 (1998) 27.
[10] G.W. Smith, Mater. Res. Soc. Symp. Proc. 481 (1998) 327.
[11] G.W. Smith, Thermochim. Acta 317 (1998) 7.
[12] G.W. Smith, Thermochim. Acta 323 (1998) 123.
[13] S. Yannacopoulos, S.O. Kasap, J. Mater. Res. 5 (1990) 791.
[14] V. Kwong, Y.C. Koo, S.J. Thorp, K.T. Aust, Acta Metall. Mater. 39 (1991) 1563.
[15] R. Busch, Y.J. Kim, W.L. Johnson, J. Appl. Phys. 77 (1995) 4039.
[16] R. Busch, S. Schneider, A. Peker, W.L. Johnson, Appl. Phys. Lett. 67 (1995) 1544.
[17] S. Spriano, C. Antonione, R. Doglione, L. Battezzati, S. Cardoso, J.C. Soares, M.F. da Silva, Phil. Mag. B 76 (1997) 529.
[18] T. Ozawa, J. Therm. Anal. 2 (1970) 301.
[19] C. Badini, F. Marino, E. Verne, Mater. Sci. Eng. A 191 (1995) 185.
[20] Perkin-Elmer Corp., Norwalk, CT.